Contents lists available at ScienceDirect

Biophysical Chemistry

Optical investigation of the electron transfer protein azurin–gold nanoparticle system

Ines Delfino *, Salvatore Cannistraro

Biophysics and Nanoscience Centre, CNISM, Facoltà di Scienze, Università della Tuscia, Viterbo, Italy

ARTICLE INFO

ABSTRACT

The hybrid system obtained by conjugating the protein azurin, which is a very stable and well-described protein showing a unique interplay among its electron transfer and optical properties, with 20-nm sized gold nanoparticles has been investigated. Binding of azurin molecules to gold nanoparticle surface results in the red shift of the nanoparticle resonance plasmon band and in the quenching of the azurin single tryptophan fluorescence signal. These findings together with the estimate of the hydrodynamic radius of the composite, obtained by means of Dynamic Light Scattering, are consistent with the formation of a monolayer of protein molecules, with preserved natural folding, on nanoparticle surface. The fluorescence quenching of azurin bound molecules is explained by an energy transfer from protein to metal surface and it is discussed in terms of the involvement of the Az electron transfer route in the interaction of the protein with the nanoparticle.

© 2008 Elsevier B.V. All rights reserved.

1. Introduction

Integrating biological molecules with nanoparticles into hybrid devices permits to combine natural biomolecule functions, such as catalysis, recognition and electron transfer, with the unique electronic, optical, and catalytic properties of nanoparticles, arising from their reduced dimension and high surface-to-volume ratio [1–3]. Noble metal nanoparticles exhibit a strong surface plasmon resonance absorption, due to electron collective oscillations, which is responsible for their brilliant colour and is highly dependent on particle size and surface environment [4,5]. The plasmon resonance can also be involved in a modulation of the electric field around the nanoparticle, giving rise to the enhancement of Raman scattering or fluorescence signal of nearby molecules [6,7]. Moreover, when biomolecules are conjugated with nanoparticles, the mixing of their energy levels has been shown to favour the occurrence of either energy transfer or electron transfer phenomena [7,8]. In this way, it is possible to study fundamental processes characterizing the interaction of metal nanoparticles with organic or biological molecules [4,9,10]. Furthermore, nanoparticle properties can be exploited for realizing nano-hybrid systems for various applications, also thanks to the possibility to suitably design their characteristics with a proper selection of the employed biotic element [3,11–13].

In this framework, electron transfer (ET) proteins are attracting growing interest. In particular, azurin (Az) is one of the most promising ET proteins because of its very peculiar properties and its capability to form molecular complexes with natural partners (i.e., cytochrome c551) [14,15] and other biomolecules (i.e., p53) [16,17], as recently outlined. It belongs to the class of redox blue copper proteins acting as electron shuttles in many important biological reactions, for instance in photosynthesis and in bacterial respiratory redox-chains [18–20]. They are endowed with very efficient ET mechanisms which occur at the level of single electron, even over long distances, in a very fast, directional way [21] and can be gated by proper modulation of the applied potential [22]. Az ET process proceeds via the copper (Cu(II))-containing active site which is characterized by an intense ligand-to-metal-charge transfer (LMCT) absorption band located at 628 nm [23,24]. Interestingly, it has been shown that an electron transfer well mimicking the thermal one can be induced by light irradiating Az in its LMCT band [25], similarly to other blue copper proteins [26–28], pointing out an intriguing interplay between Az optical and electrical properties. Additionally, Az ET path is hypothesized to involve the protein single tryptophan residue [29], an intrinsic fluorophore located at position 48 (Trp48) in a highly hydrophobic environment [30,31], which is very sensitive to protein conformation [30–32].

The integration of a biotic element with such extraordinary and versatile abilities into a nanoparticle-based hybrid system holds potential for a variety of applications ranging from bio-optoelectronics (for designing, as examples, biomemories, optical switches, data storage systems) [33,34] up to biomedicine, by taking advantage, for example, of Az capability to recognize biomolecular analytes as disease markers [16,17]. However, this potential could be fully exploited only once the basic properties of Az-based nano-hybrid systems have been described and their connection with the interaction occurring at the interface have been explored.

In this paper, we report on an optical spectroscopy study of the system obtained by conjugating the protein Az to gold nanoparticles (AuNPs) aiming at a deeper knowledge of both the interactions of protein with nanoparticles and the resulting photophysical properties of

* Corresponding author. Tel.: +39 0761 357026; fax: +39 0761 357027.
E-mail addresses: delfino@unitus.it (I. Delfino), cannistr@unitus.it (S. Cannistraro).

the hybrid system. Results from fluorescence and absorbance spectroscopy along with Dynamic Light Scattering (DLS) measurements are discussed in the view of the formation of a protein monolayer on nanoparticle surface and of potential involvement of the protein ET site in the interaction between the protein and the metal surface.

2. Experimental methods

Az from *Pseudomonas aeruginosa* was purchased from Sigma Aldrich Chemical Co. and used without further purification (20-nm sized). AuNP solution was purchased from Ted Pella Inc., the concentration of commercial solution being 1.13 nM in AuNPs.

Stock Az solution was prepared by dissolving the protein in MilliQ water (Millipore 18 MΩ cm) at a concentration of 100 μM. This solution was further diluted in water or in AuNP solution in order to obtain samples at different Az concentrations with and without AuNPs. In particular, for absorption and fluorescence spectroscopy measurements, Az+AuNP solutions at [AuNP]=1.02 nM and Az concentrations ranging from 0.7 up to 11 μM were investigated. Difference absorption measurements were carried out on Az+AuNP solutions at [Az]=8 and 14 μM and AuNP concentrations in 0.022–0.20 nM range. DLS measurements were performed on 1.02-nM AuNP solutions with ([Az]=11 μM) and without Az.

Optical absorbance and difference absorbance spectra were recorded at room temperature by a double beam Jasco V-550 UV/visible spectrophotometer by using 1-cm path length cuvettes and 2-nm bandwidth. The investigated spectral range was 250–800 nm. Absorbance spectra were collected using MilliQ water as reference. For the acquisition of difference absorbance spectra, the cuvette containing the Az+AuNP solution was placed on the sample beam path, while a cuvette filled with an AuNP solution was on the reference path, the two solutions (sample and reference) being at the same AuNP concentration.

DLS measurements [35] were taken at room temperature by using a θ=90° scattering geometry and an Ar laser light source (Ion Laser Technology Inc.) running at 488 nm (20 mW). The scattered light was detected by a photomultiplier and then passed to a BI-9000 (Brookhaven Instruments) digital correlator with a sampling time range of 0.1 μs to 1000 ms. The temperature of the sample was kept at 25.0±0.5 °C by a thermostatic bath. The scattering intensity data were processed using the BI 9000 software in order to obtain the hydrodynamic diameter and the size distribution of the scatterers in each sample. Experiment duration was in the range of 5–10 min, and each experiment was repeated several times on freshly prepared solutions.

Steady-state fluorescence emission spectra, following 280- and 290-nm excitations, were collected at room temperature in the range 290–450 nm (or 300–450 nm) by a Spex FluoroMax (Jobin Yvon, France) spectrofluorometer, equipped with 450 W Xenon lamp and two monochromators. The band-pass width for the excitation and emission monochromators was 5 nm. An integration time of 1.0 s, that relates to 0.5 nm step, was used. The light emitted by 400 μl of sample kept in a 0.2×1.0 cm internal size quartz cuvette was collected at right angle to the excitation radiation. Fluorescence spectra of reference samples were always recorded and subtracted from the experimental data to correct for background. The spectra were also corrected for variations in lamp intensity by dividing the sample signal intensity by the reference (Spex photodiode detector) intensity. A correction for Inner Filter Effect was introduced, because of the high absorption due to AuNP solution in the investigated region, according to [31]

$$F_{corr} = F_{meas} \cdot 10^{(A_{ex}+A_{em}/5)/2} \tag{1}$$

where F_{corr} and F_{meas} are measured and corrected fluorescence emission spectra, respectively, and A_{ex} and A_{em} are the absorbance of the AuNP solution at excitation and emission wavelengths, respectively. A_{em} is divided by a factor 5 for taking into account the cuvette geometry.

Scattering effects on emission spectra were neglected because of the high ratio between absorption and scattering cross-sections [4,5].

3. Results and discussion

3.1. Absorption

Representative absorption spectra of Az and Az+AuNP water solutions are shown in Fig. 1 along with the corresponding spectrum of bare AuNP solution. The absorption spectrum of the Az solution (continuous black line) shows two main peaks located at 280 and 628 nm. The former is due to the presence of the aromatic residues, including the lone tryptophan (Trp48) [30,31]. The latter is typical of a type-1 blue copper protein and is assigned to the LMCT transition (S(Cys-π)→Cu(II) $d_{x^2-y^2}$), involving the copper atom of the active site and one of the five metal ligands (specifically, Cys112) [23,24]. An intense plasmon resonance band, peaking at 522 nm, is evident in the absorption spectrum of the AuNP solution (continuous gray line). Plasmon resonance bands have been widely studied and they are now recognized to arise from the superposition of all contributing multi-pole oscillations peaking at different energies [4,5]. The frequency and width of the surface plasmon absorption bands depend on the size and the shape of metal nanoparticles as well as on the dielectric constant of metal itself and surrounding medium. In the present case, the features of the plasmon absorption band shown in Fig. 1 are consistent with a solution of 20-nm sized gold spherical particles, in agreement with the manufacturer specifications.

The spectrum of Az+AuNP solution (Fig. 1, dashed line) is dominated by the AuNP plasmon resonance band, being the signal due to Az very small (see absolute absorbance of dashed and continuous black-line spectra of Fig. 1, reflecting the extinction coefficient values). This band is slightly shifted at higher wavelengths with respect to AuNP solution without Az (Az-free). This shift depends on Az concentration as it is clear from Fig. 2, where the normalized absorption spectra of Az+AuNP solutions at different Az concentrations are shown along with a zoom of the wavelength region of plasmon band peaks (inset). A multi-peak Gaussian fitting procedure points out that red shift and width (FWHM) of the peak increase as long as the Az concentration increases, until a maximum value is reached. The trend of the peak position as a function of Az concentration is shown in Fig. 3. At the highest investigated Az concentration value (11 μM), the plasmon band has experienced a small but consistent red shift (6 nm). The plasmon band is also broadened by 7 nm, which corresponds to a bandwidth increase of 230 cm^{-1} on a frequency scale.
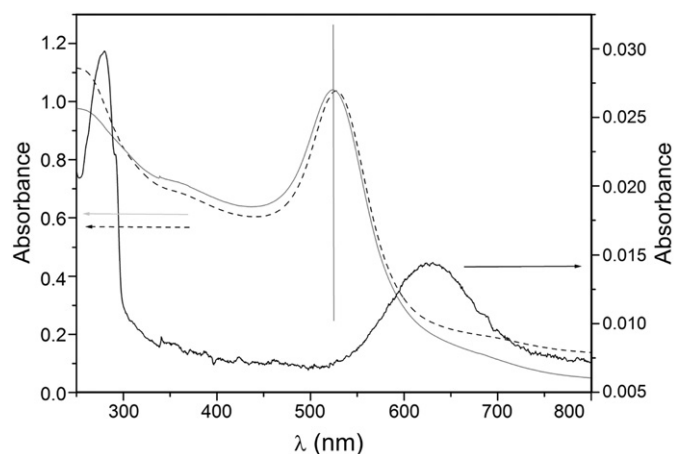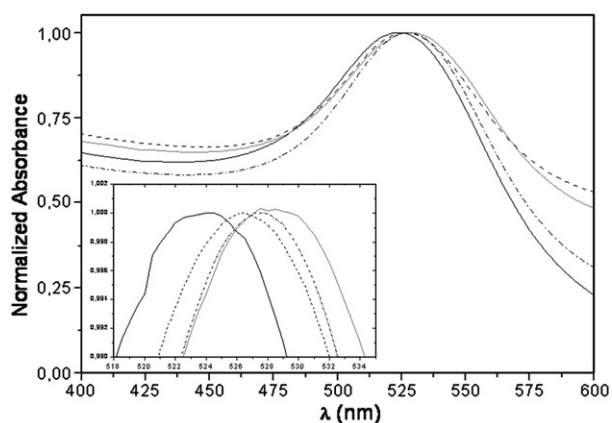

Fig. 1. Absorption spectra of Az solutions ([Az]=2.8 μM) with (dashed line) and without (continuous black line) 20-nm sized AuNPs ([AuNP]=1.02 nM). For comparison, absorption spectrum of 1.02-nM bare AuNP solution is shown (continuous gray line). For dashed black line and continuous gray line the vertical scale is on the left; for continuous black line it is on the right.

Fig. 2. Normalized absorption spectra of Az + AuNP solutions at [AuNP] = 1.02 nM and various Az concentrations: 0 μM (continuous black line), 0.7 μM (dotted black line), 2.8 μM (dashed black line), 11 μM (continuous gray line). Inset: Zoom of the wavelength region of plasmon resonance band peaks.

It has been reported that the analysis of the overall characteristics of the plasmon band can be exploited to elucidate phenomena occurring at nanoparticle interface, including bioconjugation and molecular recognition [10,36]. Accordingly, three factors can be invoked as possible causes of the plasmon band shift and/or broadening detected in the absorption spectra of Az + AuNP solutions: (a) aggregation of nanoparticles upon bioconjugation, (b) electronic communication between the Az redox center and the gold nanoparticle, and (c) changes in local dielectric environments. The hypothesis of aggregation caused by Az addition can be reasonably ruled out by considering the absorbance spectra. In fact, aggregation of AuNPs would have lead to the formation of (at least) 40-nm sized clusters and, thus, to a red shift of the plasmon resonance band larger than that outlined in Az + AuNP solution absorption spectra (see Fig. 2). Moreover, the hypothesis of aggregation caused by Az addition has been definitely ruled out by DLS results showing no evidence for the presence of aggregates of two or more AuNPs in the investigated AZ + AuNP solutions (scatterer size distribution is discussed in the following). The other two hypotheses are plausible and consistent with the direct interaction between gold surface and Az molecules. In case (b), interfacial ET from the excited Au plasmon to the bound Az molecules could shorten the lifetime of the plasmon excited state, leading to a corresponding bandwidth increase. This process has recently emerged as an attractive interpretation for the origin of the observed AuNP plasmon band shift and broadening upon conjugation with cytochrome *c* [10]. However, the occurrence of the process has not been definitely demonstrated. To get deeper insight into the role of Az active site (and, hence, into the occurrence of an interfacial ET process) in the interaction between Az and AuNP, the occurrence of potential modifications of Az LMCT band upon AuNP addition by means of difference absorption measurements has been investigated. Our data (not shown) indicate that this band remains unperturbed when AuNPs are added, thus suggesting that no changes take place in copper oxidation state. However, because the extinction coefficient of AuNP plasmon band (10^9 M^{-1} cm^{-1}) greatly exceeds that of Az at 628 nm (5000 M^{-1} cm^{-1}), the experiments have been carried out in solution with an excess of Az with respect to AuNP. In fact, in order to obtain a reliable difference spectrum with well defined LMCT band, it was necessary to work with high Az concentrations (8 and 14 μM in our experiments) and low AuNP concentrations (ranging from 0.022 to 0.20 nM) and, consequently, it cannot be excluded that the possible changes induced in LMCT absorption band by the interaction of Az with AuNP are hidden by signal from Az molecules not interacting with gold nanoparticles. In case (c), the presence of Az near AuNP could cause significant changes in the local dielectric environment of the nanoparticle according to the well-known single particle plasmon band red shift

with increasing medium dielectric constant [9,37]. Notably, the experimental characteristics of the AuNP plasmon band after Az addition are consistent with Mie prediction for a 20-nm diameter gold sphere coated with a uniform Az monolayer having the same optical and geometrical properties of an Az monolayer formed on a flat substrate (properties of the monolayer have been extracted from Ref. [38]). In fact, the predicted Mie extinction spectrum, in the visible range, obtained by means of a dedicated software based on a well-known algorithm [39], shows a plasmon band shifted at 527 nm and broadened up to 70 nm in fairly good agreement with the corresponding values extracted from the absorption spectrum of the solution with the highest Az concentration (band peaked at 528 nm with a FWHM of 66 nm). This suggests that the changes in plasmon band features upon Az addition are due to local dielectric environment modification connected to direct interaction of the Az molecules with gold surface leading to the formation of a (mono) layer of Az molecules bound to AuNP surface. This hypothesis well relates with the well-known ability of Az to link gold surfaces, as also theoretically described by means of molecular dynamics simulations [15,40–42]. Whatever the link is, if a monolayer is formed, an estimate of the theoretical number of Az proteins (N_{Az}) that each spherical particle can accomodate on its surface may be derived from steric considerations using the following expression [43]:

$$N_{Az} = 0.65 \cdot \left(\frac{R_T^3 - R_{AuNP}^3}{R_{Az}^3} \right) \tag{2}$$

where R_{AuNP} is the AuNP radius (10 nm) and R_T is the radius of the AuNP plus bound Az molecules ($R_{AuNP} + 2R_{Az}$), with $R_{Az} = 2$ nm [44]. Actually, this description is valid under two assumptions: (i) Az molecules can be approximated as rigid spheres, close packed around a central sphere (AuNP); (ii) the conformation of the protein interacting with the nanoparticle is not significantly perturbed. In the investigated Az + AuNP system, both the assumptions can be thought to be valid since Az is known to be a quite globular protein and it is reasonable to think that it does not undergo such significant conformation changes upon the interaction with AuNP surface (however, this aspect will be discussed in the following). By introducing the expected values for our Az + AuNP system into Eq. (2), an estimate of ≈140 proteins per nanoparticle was obtained. Because of the occurrence of a close and uniform packing of proteins around an AuNP seems fairly unlikely, the previous calculation has to be viewed as a maximum theoretical limit of conjugation, and thus, as a maximum number of linking sites per nanoparticle. This implies the presence, in the investigated solutions, of a number of Az molecules greater than that needed to form a monolayer on each gold nanoparticle.
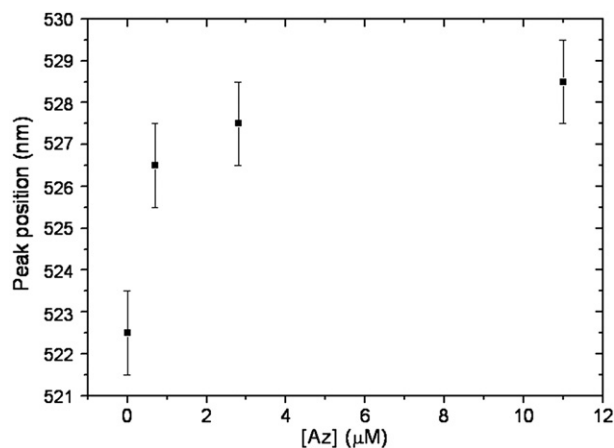
Fig. 3. Dependence of position of plasmon resonance band peak on Az concentration as obtained by multi-peak Gaussian fitting procedure performed on spectra shown in Fig. 2.
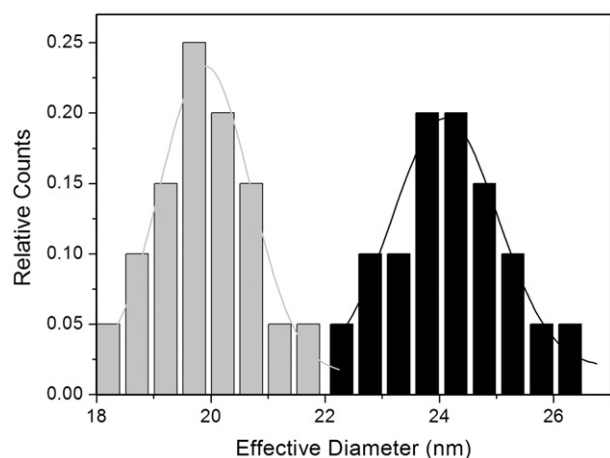
Fig. 4. Size distribution of AuNP in solution (at [AuNP] = 1.02 nM) before and after Az addition, as obtained by the analysis of DLS results; gray bars being referred to bare AuNP solution and black bars to Az+AuNP solution ([Az] = 11 μM). Continuous lines represent the results of a Gaussian fit procedure (see text).

3.2. Dynamic Light Scattering

The size distributions of AuNPs in solution before and after Az addition, as obtained by the analysis of DLS results [35], are shown in Fig. 4 (gray and black bars, respectively). They point out that diameters of the bare AuNP range from 18 to 22 nm and those of Az+AuNP systems range between 22 and 27 nm. A Gaussian fit procedure performed on both the outlined distributions (results are shown as continuous lines in the figure) gives the best estimation of the sizes, being 19.9 ± 1.6 nm for Az-free solution and 24.1 ± 1.8 nm when an excess of Az is added to AuNP-containing solutions.

The increase in scatter (AuNP) size upon Az addition confirms that Az molecules have grafted on gold nanoparticles. Comparing the diameters of Az+AuNP and bare AuNP can determine how far the Az molecule protrudes from the AuNP surface. The difference between the two mean diameters is about 4 nm, which can be thought as twice the apparent thickness of the shell coating the AuNP. This estimate is consistent with the thickness of an Az monolayer on planar gold [15], thus confirming the formation of an Az monolayer on AuNP surface. Therefore, the Az+AuNP system can be thought as a 20-nm sized gold nanoparticle with a 2-nm shell composed by less than 140 Azurin molecules around it, as sketched in Scheme 1.

3.3. Fluorescence

Representative fluorescence emission spectra, following a 280-nm excitation, of Az and Az+AuNP solutions are shown in Fig. 5. Az solution emission spectrum (continuous line) shows the well-known broad peak with a maximum at 308 nm due to the single buried tryptophan (Trp48) [29,30]. Fluorescence spectrum of Az+AuNP
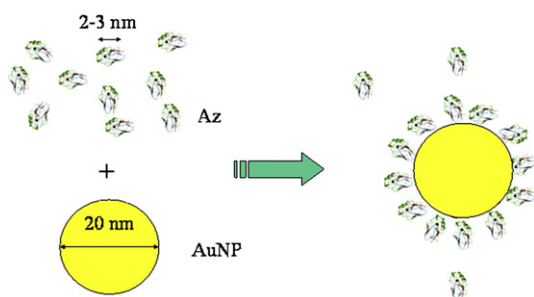
**Scheme 1.** Formation of Az monolayer on gold nanoparticles.
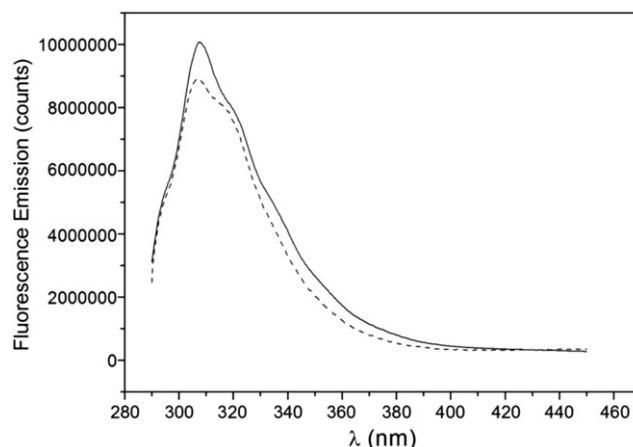
Fig. 5. Representative fluorescence emission spectra of Az (continuous line) and Az+AuNP (dashed line) solutions at [Az] = 2.8 μM and [AuNP] = 1.02 nM.

solution (dashed line) is dominated by signal due to Az, since 20-nm sized AuNPs are known to have negligible fluorescence signal in the investigated region [45], as we have also observed. The addition of AuNPs to Az solutions results in (i) a preservation of the shape of the spectrum and (ii) a slight decrease of the Az emission intensity, suggesting the occurrence of fluorescence quenching process since the spectra have been corrected for trivial intensity effects. In fact, the analysis of the shape of Trp emission spectrum can provide useful information about the changes of the protein conformational state, fluorescence emission spectrum of the Trp residue in a protein being closely related to its solvent exposure [31,32]. In particular, it was shown that when unfolding process occurs in Az molecules, 308-nm emission peak shifts up to 357 nm as a consequence of an increased exposition of the Trp [46]. Accordingly, the outlined preservation of the shape of the emission spectrum upon AuNP addition in our experiments is an indication that Az molecules participating to the signal (and, thus, also the molecules bound to AuNP surface) remain presumably in their native configuration. This is in agreement with both experimental results [15,41] and molecular dynamics simulation of an Az molecule near a gold surface showing that the protein under-goes only small configurational changes even when it is covalently bound to the surface [42].

The examination of the dependence of Az+AuNP solution fluorescence intensity on Az concentration has to be carried out by taking into account that we are interested in the variation of fluorescence signal occurring as a consequence of the AuNP addition. Considering that changes are expected to arise only from bound Az molecules and that the amount of free Az molecules in each solution is dependent on Az concentration, the ratio $\frac{F_0-F}{F_0}$, where F_0 is the integrated fluorescence emission of Az solution and F is the same for the corresponding Az+AuNP solution, has been analysed to better evidence signal variation. Accordingly, in Fig. 6, $\frac{F_0-F}{F_0}$ is shown as a function of the ratio of theoretical maximum number of binding sites (from Eq. (2), $N_s = 140*[AuNP]*N_A$, where N_A is the Avogadro number) to total number of Az molecules available in the investigated sample ($N_{tAz} = [Az]*N_A$). An increase in the relative difference of fluorescence intensities as the ratio N_s/N_{tAz} increases is obtained till a maximum quenching (≈20%) is reached, for $N_s/N_{tAz} > ≈ 10\%$. This behaviour is consistent with a dependence of the total quenching on the number of bound Az, resulting from a direct interaction of Az molecule with nanoparticle gold surface. Under the assumption of the formation of Az monolayer on gold nanoparticle, the signal of Az molecules belonging to the monolayer can be supposed to be the only actually quenched, while free Az molecules preserve their fluorescence intensity. The total fluorescence is obviously due to the sum of signal of quenched and not quenched sources. Accordingly, as the relative
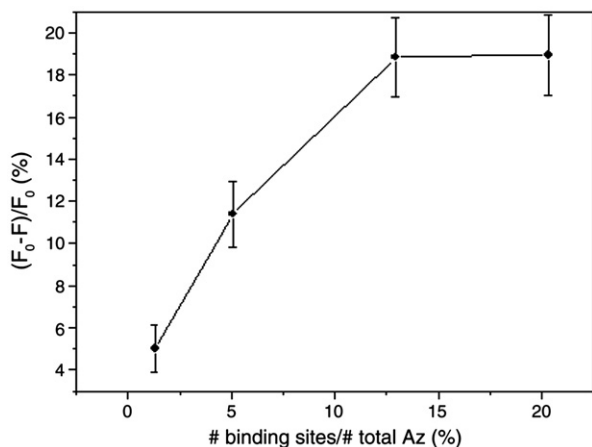
Fig. 6. $(F_0-F)/F_0$ vs (# binding sites, N_s)/(# total Az molecules, N_{tAz}) as obtained by considering integrated emission for the all investigated Az solutions (continuous line being a guide for the eye).

number of free Az molecules (not quenched) increases, the overall quenching efficiency seems to be reduced. In the following discussion, we reasonably assume that: (i) the extinction coefficient in the UV range is the same for free and bound Az molecules; (ii) the quantum yield of the free Az, Q_0, remains unchanged upon AuNP addition; (iii) the quantum yield of Az molecules bound to gold surface, Q, is the same for all the bound molecules and $Q<Q_0$ since a reduction of fluorescence signal has been detected. In this frame, F_0 and F can be defined as: $F_0=Q_0N_{tAz}$ for Az solution without AuNPs (N_{tAz}, the total number of Az molecules available in the solution, being equal, at fixed Az concentrations, for solutions containing or not AuNPs), and $F=QN_{bAz}+Q_0N_{frAz}$ for Az+AuNP solution, where N_{bAz} is the number of Az molecules bound to gold surface in Az+AuNP solution, and N_{frAz} is the number of Az molecules left not bound (free) in that solution. By introducing the condition $N_{frAz}=N_{tAz}-N_{bAz}$, the following equation is obtained:

$$\frac{F_0-F}{F_0} = \left(\frac{Q_0-Q}{Q_0}\right)\frac{N_{bAz}}{N_{tAz}} \tag{3}$$

which explains the relationship between the experimental signal and the number of bound Az molecules. Obviously, N_{bAz} depends on the adsorption processes of the molecule (Az) onto the surface (AuNP's), but for $N_{tAz} \gg N_{bAz}$, that is at high Az concentrations and low N_{bAz}/N_{tAz}, we can roughly consider $N_{bAz}/N_{tAz} \propto N_s/N_{tAz}$. In these conditions, Eq. (3) qualitatively describes the linear dependence of $\frac{F_0-F}{F_0}$ on N_s/N_{tAz} outlined in Fig. 6 for $N_s/N_{tAz}<\approx10\%$, while, behind this threshold value, $\frac{F_0-F}{F_0}$ remains unchanged upon reducing the total number of Az molecules. This saturation effect has to be ascribed to the existence of a minimum N_{bAz}/N_{tAz} ratio, which is related to the adsorption equilibrium.

These results confirm that Az molecules bound to gold surface experience a quenching process, i.e. a decrease of quantum yield as compared to that of free Az molecules. In order to better understand such process, it is useful to express the quantum yield of free (Q_0) and bound Az (Q) molecules as [31]

$$\text{a) } Q_0 = \frac{k_r}{k_r + k_{nr}}; \quad \text{b) } Q = \frac{k_r'}{k_r' + k_{nr}'} \tag{4}$$

where k_r and k_{nr} are the rate of radiative and nonradiative decays for Az-free molecule, respectively, and k_r' and k_{nr}' are the same for Az bound molecule.

Actually, the reduction of the quantum yield of a fluorophore in the proximity of a metallic nanoparticle has been reported for various fluorophores. Experimental and theoretical studies have demonstrated

that the effect is ascribed to both reduction of radiative decay rate ($k_r'<k_r$) and increase of nonradiative rate ($k_{nr}'>k_{nr}$), being the relative extent of the phenomena dependent on both nanoparticle size and distance between metal surface and fluorophore [47–50]. In the Az+AuNP system, the decrease of the fluorophore radiative decay rate (thus, $k_r'<k_r$) can be ascribed to the so-called phase induced radiative rate suppression, occurring when the molecular dipole and the dipole induced on the AuNP radiate out of phase if the molecules are oriented tangentially to the AuNP surface, leading to a destructive interference [48]. The lack of a preferential orientation of Az molecules with respect to the nanoparticle surface suggests that this orientation-dependent effect cannot fully explain the outlined fluorescence quenching of bound Az molecules. The characteristics of the investigated system suggest that an important role in fluorescence quenching is played by nonradiative decay rate increase, which is thought to be induced by the opening of an additional nonradiative decay path connected to electron and/or energy transfer processes [47,49,51,52] (in such cases, the total nonradiative rate would be $k_{nr}'+k_T$, where k_T is the transfer decay rate, hence, the denominator in Eq. (4b) becoming $k_r'+k_{nr}'+k_T$). In fact, on one hand, the injection of a charge from the fluorophore excited state to the metal surface provides the additional nonradiative decay route that, in specific conditions, can compete with the naturally available de-excitation processes [49,52]. Actually, such a process is known to depend on the fluorophore-metal energy level interplay, on the surface properties and on the distance between protein and metal surface, being more probable for shorter distances. On the other hand, a nonradiative decay rate increase can be due to the occurrence of a Resonance Energy Transfer (RET) process [47,51], a peculiar energy transfer occurring whenever the emission spectrum of a fluorophore, called the donor, overlaps with the absorption spectrum of another molecule, called the acceptor. The donor–acceptor distance has to fall within 1–10 nm, values generally reported in the literature for an efficient energy transfer process [31]. In the Az+AuNP complex, a direct RET between Trp (of bound Az molecules) and gold nanoparticle can be thought to occur, being the Trp the donor and the nanoparticle the acceptor. In fact, absorption and emission spectra of AuNPs and Az are overlapping (see Fig. 7) and the Trp is supposed to be inside the protein monolayer coating the AuNP (thus, is far from the metal surface less than 3 nm). Actually, RET efficiency is dependent on the donor–acceptor distance, but it has been shown that the outlined experimental dependence is much weaker than expected from theoretical predictions [48]. Another intriguing process involving energy transfer could be invoked to explain the outlined quenching effect. Theoretical work [53] and very recent experimental studies [7,50] have shown that metal particles could increase the efficiency of a naturally occurring RET between a donor and an acceptor when they are
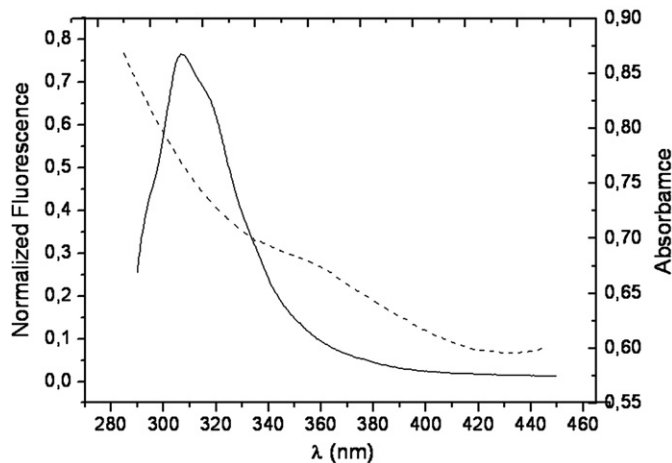
Fig. 7. Overlap between Az emission spectrum (continuous line) and absorption spectrum of AuNP solution (dashed line).

close to a metal particle, leading to the so-called RET enhancement. It is well known that in Az, Trp fluorescence signal is dramatically increased when Cu is removed, thus Cu itself is thought to operate as fluorescence quencher. Facile energy transfer between the Trp and the Cu-ligand complex is thought to be responsible for the fluorescence quenching in Trp. Presumably, this quenching occurs between the Trp $^1L_{ab}$ states and a Cu-ligand charge transfer state [54]. The quenching of Trp fluorescence upon conjugation with AuNPs can be due to an enhancement of this naturally occurring energy transfer process. The energy transfer-based hypothesis of fluorescence quenching in Az+AuNP system is in agreement with very recent studies on quenching of fluorescence from Bovine Serum Albumin molecules bound to gold nanoparticles [55]. Interestingly, in the peculiar case of Az+AuNP system, the occurrence of an energy transfer between Trp and gold could be indicative of some changes occurring in the electron transfer path and, thus, in protein conductive properties, when Az is in the vicinity of an AuNP since there are strong indications that the main electron transfer route in Az is a path through the buried Trp48 [29] and that Trp participates to electron transfer in biological redox machines [56].

4. Conclusions

The optical spectroscopic study on the hybrid system obtained by conjugating the electron transfer blue copper protein Az to 20-nm sized AuNPs provided interesting information on the interactions occurring at the interface between the protein and the metal surface and on the resulting photophysical properties of the system. The analysis of the plasmon resonance band of the composite along with DLS results confirmed the interaction of Az with gold surface, probably involving a monolayer of protein molecules grafted on AuNPs. Each nanoparticle was estimated to bind at maximum 140 Az molecules which were thought to preserve their natural folding. The investigation of fluorescence emission spectrum of Az+AuNP system, due to Az single buried Trp, outlined the occurrence of a quenching effect related to protein–nanoparticle interactions. This intriguing phenomenon was explained by the increase of the nonradiative decay rate as a consequence of a direct energy transfer between Trp and gold surface or to the enhancement of the naturally occurring energy transfer between Trp and Cu-ligand site, thus suggesting the involvement of the ET path in the interactions between Az and gold surface.

These results enable a step forward the exploitation of the potentialities of Az-based nano-hybrid systems which deserve interest for a variety of applications ranging from bio-optoelectronics up to biomedicine.

Acknowledgement

References

[1] C.M. Niemeyer, Nanoparticles, proteins, and nucleic acids: biotechnology meets materials science, Angew. Chem., Int. Ed. 40 (2001) 4128–4158.
[2] H. Gu, K. Xu, C. Xu, B. Xu, Biofunctional magnetic nanoparticles for protein separation and pathogen detection, Chem. Commun. (2006) 941–946.
[3] Q. Huo, A perspective on bioconjugated nanoparticles and quantum dots, Colloids Surf. B: Bionterfaces 59 (2007) 1–10.
[4] S. Link, M.A. El-Sayed, Shape and size dependence of radiative, non-radiative and photothermal properties of gold nanocrystals, Int. Rev. Phys. Chem. 19 (2000) 409–453.
[5] P.V. Kamat, Photophysical, photochemical and photocatalytic aspects of metal nanoparticles, J. Phys. Chem. B 106 (2002) 7729–7744.
[6] K. Kneipp, H. Kneipp, I. Itzkan, R.R. Dasari, M.S. Feld, Ultrasensitive chemical analysis by Raman spectroscopy, Chem. Rev. 99 (1999) 2957–2975.
[7] J.R. Lakowicz, J. Kusba, Y. Shen, J. Malicka, S. D'Auria, Z. Gryczynski, I. Gryczynski, Effects of metallic silver particles on resonance energy transfer between fluorophores bound to DNA, J. Fluoresc. 13 (2003) 69–77.
[8] I. Willner, R. Baron, B. Willner, Integrated nanoparticle-biomolecule systems for biosensing and bioelectronics, Biosens. Bioelectron. 22 (2007) 1841–1852.
[9] P.K. Jain, W. Huang, M.A. El-Sayed, On the universal scaling behavior of the distance decay of plasmon coupling in metal nanoparticle pairs: a plasmon ruler equation, Nano Lett. 7 (2007) 2080–2088.
[10] P.S. Jensen, Q. Chi, F.B. Grumsen, J.M. Abad, A. Horsewell, D.J. Schiffrin, J.J. Ulstrup, Gold nanoparticle assisted assembly of a heme protein for enhancement of long-range interfacial electron transfer, J. Phys. Chem. C. 111 (2007) 6124–6132.
[11] I.H. El-Sayed, X. Huang, M.A. El-Sayed, Surface plasmon resonance scattering and absorptin of anti-EGFR antibody conjugated gold nanoparticles in cancer diagnostics: applications in oral cancer, Nano Lett. 5 (2005) 829–834.
[12] N.L. Rosi, C.A. Mirkin, Nanostructures in biodiagnostics, Chem. Rev. 105 (2005) 1547–1562.
[13] I. Willner, B. Willner, E. Katz, Biomolecule-nanoparticle hybrid systems for bio-electronic applications, Bioelectrochemistry 70 (2007) 2–11.
[14] M.M. Hervás, J.A. Navarro, A. Díaz, H. Bottin, M.A. De La Rosa, Laser flash kinetic analysys of the fast electron transfer from plastocyanin and cytochrome c6 to photosystem I. Experimental evidence on the evolution of the reaction mechanism, Biochemistry 34 (1995) 11321–11326.
[15] B. Bonanni, D. Alliata, L. Andolfi, A.R. Bizzarri, S. Cannistraro, Redox metal-loproteins on metal surface as hybrid system for bionanodevices: an extensive characterization at the single molecule level, in: C.P. Norris, (Ed.), Surface Science Research Developments, Nova Science Publishers, Inc., New York, 2005, pp. 1–73.
[16] Y. Hiroaka, T. Yamada, M. Goto, T.K. Das Gupta, A.M. Charkrabarty, Modulation of mammalian cell growth and death by prokaryotic and eukaryotic cytochrome c, Proc. Natl. Acad. Sci. [USA] 101 (2004) 6427–6432.
[17] V. De Grandis, A.R. Bizzarri, S. Cannistraro, Docking study and free energy simulation of the complex between p53 DNA-binding domain and azurin, J. Mol. Recognit. 20 (2007) 215–226.
[18] A.G. Sykes, Active-site properties of the blue copper proteins, Adv. Inorg. Chem. 36 (1991) 377–408.
[19] E.I. Solomon, M.J. Baldwin, M.D. Lowery, Electronic structures of active sites in copper proteins: contributions to reactivity, Chem. Rev. 92 (1992) 521–542.
[20] C. Dennison, Investigating the structure and function of cupredoxins, Coord. Chem. Rev. 249 (2005) 3025–3054.
[21] A.R. Bizzarri, S. Cannistraro, Electron transfer in metalloproteins, in: G. Bassani, G. Liedl, P. Wyder (Eds.), Encyclopedia of Condensed Matter Physics, Elsevier, Amsterdam, The Netherlands, 2005, pp. 361–369.
[22] W. Haehnel, T. Jansen, K. Gause, R.B. Klösgen, B. Stahl, D. Michl, B. Huvermann, M. Karas, R.G. Hermann, Electron transfer from plastocyanin to photosystem I, EMBO J. 13 (1994) 1028–1038.
[23] E.I. Solomon, J.W. Hare, D.M. Dooley, J.H. Dawson, P.J. Stephens, H.B. Gray, Spectroscopic studies of stellacyanin, plastocyanin, and azurin. Electronic structure of the blue copper sites, J. Am. Chem. Soc. 102 (1980) 168–178.
[24] E. Fraga, M.A. Webb, G.R. Loppnow, Excited-state charge-transfer dynamics of azurin, a blue copper protein, from resonance Raman intensities, J. Phys. Chem. B 101 (1996) 5062–5069.
[25] T. Cimei, A.R. Bizzarri, S. Cannistraro, G. Cerullo, S. De Silvestri, Vibrational coherence in azurin with impulsive excitation of the LMCT absorption band, Chem. Phys. Lett. 362 (2002) 497–503.
[26] M.D. Edington, W.M. Diffey, W.J. Doria, R.E. Riter, W.F. Beck, Radiationless decay from the ligand-to-metal charge-transfer state in the blue copper protein plastocyanin, Chem. Phys. Lett. 275 (1997) 119–126.
[27] L.D. Book, D.C. Arnett, H. Hu, N.F. Scherer, Ultrafast pump-probe studies of excited-state charge-transfer dynamics in blue copper proteins, J. Phys. Chem. A 102 (1998) 4350–4359.
[28] I. Delfino, C. Manzoni, K. Sato, C. Dennison, G. Cerullo, S. Cannistraro, Ultrafast pump-probe study of excited-state charge-transfer dynamics in umecyanin from horseradish root, J. Phys. Chem. B 110 (2006) 17252–17259.
[29] O. Farver, L.K. Skov, S. Young, N. Bonander, B. Karlsson, T.G. Vanngard, I. Pecht, Aromatic residues may enhance intramolecular electron transfer in azurin, J. Am. Chem. Soc. 119 (1997) 5453–5454.
[30] K.K. Turoverov, I.M. Kuznetsova, V.N. Zaitsev, The environment of the tryptophan residue in Pseudomonas aeruginosa azurin and its fluorescence properties, Biophys. Chemist. 23 (1985) 79–89.
[31] J.R. Lakowicz, Principles of Fluorescence Spectroscopy, second ed.Plenum Press, New York, 1999.
[32] G. Gilardi, G. Mei, N. Rosato, G.W. Canters, A. Finazzi-Agrò, Unique environment of Trp48 in Pseudomonas aeruginosa azurin as probed by site-directed mutagenesis and dynamic fluorescence spectroscopy, Biochemistry 33 (1994) 1425–1432.
[33] D.I. Gittins, D. Bethell, D.J. Schiffrin, R.J. Nichols, A nanometre-scale electronic switch consisting of a metal cluster and redox-addressable groups, Nature 408 (2000) 67–69.
[34] T. Hugel, N.B. Holland, A. Cattani, L. Moroder, M. Seitz, H.E. Gaub, Single-molecule optomechanical cycle, Science 296 (2002) 1103–1106.
[35] I. Delfino, K. Sato, M.D. Harrison, L. Andolfi, A.R. Bizzarri, C. Dennison, S. Cannistraro, Dynamic Light Scattering, Wiley-Interscience, New York, 1976; B.J. Berne, R. Pecora, Optical spectroscopic investigation of the alkaline transition in umecyanin from horseradish root, Biochemistry 44 (2005) 16090–16097.
[36] S. Chan, M.R. Hammond, R.N. Zare, Gold nanoparticles as a colorimetric sensor for protein conformational changes, Chem. biol. 12 (2005) 323–328.
[37] P.K. Jain, M.A. El-Sayed, Surface plasmon resonance sensitivity at metal nanostructures: physical basis and universal scaling in metal nanoshells, J. Phys. Chem. C 111 (2007) 17451–17454.
[38] F. Bordi, M. Prato, O. Cavalleri, C. Cametti, M. Canepa, A. Gliozzi, Azurin self-assembled monolayers characterized by coupling electrical impedance spectroscopy and spectroscopic ellisometry, J. Phys. Chem. B 108 (2004) 20263–20272.

[39] C.F. Bohren, D.R. Huffman, Absorption and Scattering of Light by Small Particles, John Wiley & Sons, Inc., New York, 1983.

[40] L. Venkataraman, J.E. Klare, I.W. Tam, C. Nuckolls, M.S. Hybertsen, M.L. Steigerwald, Single-molecule circuits with well-defined molecular conductance, Nano Lett. 6 (2006) 458–462.

[41] J.J. Davis, H.A.O. Hill, The scanning probe microscopy of metalloproteins and metalloenzymes, Chem. Commun. 393 (2002) 200–202;
Q. Chi, J. Zhang, J.U. Nielsen, I. Friis, E.P. Chorkendorff, G.W. Canters, J.E.T. Andersen, J. Ulstrup, Molecular monolayers and interfacial electron transfer of *Pseudomonas aeruginosa* azurin on Au (111), J. Am. Chem. Soc. 122 (2000) 4047–4055.

[42] A.R. Bizzarri, Topological and dynamical properties of azurin anchored to a gold substrate as investigated by molecular dynamics simulation, Biophys. Chemist. 122 (2006) 206–214.

[43] H. Mattoussi, J.M. Mauro, E.R. Goldman, G.P. Anderson, V.C. Sundar, F.V. Mikulec, M.G. Bawendi, Self-assembly of CdSe–ZnS quantum dot bioconjugates using an engineered recombinant protein, J. Am. Chem. Soc. 122 (2000) 12142–12150;
P.P. Pompa, R. Chiuri, L. Manna, T. Pellegrino, L.L. del Mercato, W.J. Parak, F. Calabi, R. Cingolani, R. Rinaldi, Fluorescence resonance energy transfer induced by conjugation of metalloproteins to nanoparticles, Chem. Phys. Lett. 417 (2006) 351–357.

[44] H. Nar, A. Messerschmidt, R. Huber, M. Van de Kamp, G.W. Canters, Crystal structure analysis of oxidized *Pseudomonas aeruginosa* azurin at pH 5.5 and pH 9.0. A pH-induced conformational transition involves a peptide bond flip, J. Mol. Biol. 221 (1991) 765–772.

[45] J.P. Wilcoxon, J.E. Martin, F. Parsapour, B. Wiedenman, D.F. Kelley, Photoluminescence from nanosize gold clusters, J. Chem. Phys. 108 (1998) 9137–9143.

[46] P. Guptasarma, Resolving multiple protein conformers in equilibrium unfolding reactions: a time-resolved emission spectroscopic (TRES) study of azurin, Biophys. Chemist. 65 (1997) 221–228.

[47] E. Dulkeith, A.C. Mortcani, T. Niedereichholz, T.A. Klar, J. Feldmann, S.A. Levi, F.C.J.M. Van Veggel, D.N. Reinhoudt, M. Moller, D.J. Gittins, Fluorescence quenching of dye molecules near gold nanoparticles: radiative and nonradiative effects, Phys. Rev. Lett. 89 (2002) 2030021–2030024.

[48] E. Dulkeith, M. Ringler, T.A. Klar, J. Feldmann, A. Muñoz, W.J. Parak, Gold nanoparticles quench fluorescence by phase induced radiative rate suppression, Nano Lett. 5 (2005) 585–589.

[49] F. Cannone, G. Chirico, A.R. Bizzarri, S. Cannistraro, Quenching and blinking of fluorescence of a single dye molecule bound to gold nanoparticles, J. Phys. Chem. B 110 (2006) 16491–16498.

[50] J. Zhang, Y. Fu, J.R. Lakowicz, Enhanced Förster Resonance Energy Transfer (FRET) on a single metal particle, J. Phys. Chem. C 111 (2007) 50–56.

[51] B. Dubertret, M. Calame, A.J. Libchaber, Single-mismatch. detection using gold-quenched fluorescent oligonucleotides, Nat. Biotechnol. 19 (2001) 365–370.

[52] B.I. Ipe, K.G. Thomas, S. Barazzouk, S. Hotchandani, P.V. Kamat, Photoinduced charge separation in a fluorophore-gold nanoassembly, J. Phys. Chem. B 106 (2002) 18–21;
M.W. Holman, R. Liu, D.M. Adams, Single-molecule spectroscopy of interfacial electron transfer, J. Am. Chem. Soc. 125 (2003) 12649–12654.

[53] J.I. Gersten, A. Nitzan, Accelerated energy transfer between molecules near a solid particle, Chem. Phys. Lett 104 (1984) 31–37.

[54] J.A. Sweeney, P.A. Harmon, S.A. Asher, C.M. Hutnik, A.G. Szabo, UV resonance Raman examination of the azurin tryptophan environment and energy relaxation pathways, J. Am. Chem. Soc. 113 (1991) 7531–7537.

[55] L. Shang, Y. Wang, J. Jiang, S. Dong, pH-dependent protein conformational changes in albumin:gold nanoparticle bioconjugates: a spectroscopic study, Langmuir 23 (2007) 2714–2721;
N. Wangoo, C.R. Suri, G. Shekhawat, Interaction of gold nanoparticles with protein: a spectroscopic study to monitor protein conformational changes, Appl. Phys. Lett. 92 (2008) 133104/1-3.

[56] C. Shih, A.K. Museth, M. Abrahamsson, A.M. Blanco-Rodriguez, A.J. Di Bilio, J. Sudhamsu, B.R. Crane, K.L. Ronayne, M. Towrie, A. Vlcek Jr., J.H. Richards, J.R. Winkler, H.B. Gray, Tryptophan-accelerated electron flow through proteins, Science 320 (2008) 1760–1762.